Journal of Molecular Structure

Crystal structures and docking studies in cathepsin S of bioactive 1,3-diphenyl-4-(trichloro-λ4-tellanyl)but-2-en-1-one derivatives

--Manuscript Draft--

Manuscript Number:	MOLSTRUC-D-21-01523R1
Article Type:	Research Paper
Keywords:	Tellurium(IV); Crystal Structure; molecular packing; Molecular docking; cathepsin S
Corresponding Author:	Julio Zukerman-Schpector, Ph.D. Universidade Federal de Sao Carlos SãoCarlos, BRAZIL
First Author:	Julio Zukerman-Schpector, Ph.D.
Order of Authors:	Julio Zukerman-Schpector, Ph.D.
	Stella Hernandes Maganhi, PhD
	Ignez Caracelli, PhD
	Rodrigo L. O. R. Cunha, PhD
	Mauricio Angel Veja-Teijido, PhD
	Edward R.T. Tiekink, PhD
Abstract:	The molecular structures of three 1,3-diphenyl-4-(trichloro-lλ4-tellanyl)but-2-en-1-one derivatives (1–3), show similar coordination geometries defined by methylene-C, three chloride and carbonyl-O atoms. In each case, the resulting CCl3O donor set defines a square-pyramid with the vacant space opposite the methylene-C atom occupied by a lone-pair of electrons. Each of the molecules dimerises in the crystal via weak intermolecular Te…Cl interactions so a distorted ψ-pentagonal-bipyramidal geometry ensues. Previous work has shown these compounds to inhibit cathepsin S to varying extents, with 2, having 2-methoxy substituents in the 2-position of rings, being particularly effective. Molecular docking calculations of cathepsin S with ligands 1'–3' (i.e. cations derived from 1–3 by removal of one of the tellurium-bound chloride atoms) showed the higher experimental second order inactivation rate of 2, compared with the other two ligands, is explained by the observation that the ligand occludes the entrance to the channel thereby blocking access to the catalytic Cys25 site and also because 2' occupies part of the crucial subsite S3 of the protein.

Prof. Christian Jelsch
Editor,
Journal of Molecular Structure
University of Lorraine, Nancy, France

June 14th, 2021

Dear Prof. Jelsch,

We are pleased to upload a revised manuscript of our paper, now with the title "*Crystal structures and docking studies in cathepsin S of bioactive 1,3-diphenyl-4-(trichloro-λ^4-tellanyl)but-2-en-1-one derivatives*" authored by Stella Hernandes Maganhi, Ignez Caracelli, Julio Zukerman-Schpector, Rodrigo L. O. R. Cunha, Mauricio Angel Veja-Teijido and Edward R.T. Tiekink.

All the points raised by the referees were addressed as described in the file "Referees_answers_2.docx" and the corresponding changes made in the new version of the manuscript where they are highlighted.

We hope the revised manuscript meets with your Editorial requirements.

Yours sincerely,

Julio Zukerman-Schpector
(for the authors)

Reviewer #1: The present paper "Crystal structures and docking (cathepsin S) studies on bioactive trichloridotellurium(IV) 4-oxo-2,4-diphenylbutan-1-ides" reports the synthesis, crystal and docking studies of three tellurium containing compounds. The topic is highly interesting and tellurium is not frequently present in the structures of bioactive compounds, so I recommend the publication of this work after reconsideration of the following issues.

- In the title, I think it is not proper to write the target of the compounds in parenthesis between the words "docking" and "studies". The authors should modify the title.

AUTHORS' RESPONSE: As suggested, the title has been modified.

- There should be a common style to name the compounds. In the abstract, the general name of the compounds is 4-oxo-2,4-diphenylbutan-1-ide, however, it is 1,3-diphenyl-4-(trichloro-λ4-tellanyl)butan-1-one in the text. Also, the general scaffold does not contain only "butan-1-one" scaffold, the double bond in the structure needs to be mentioned.

AUTHORS' RESPONSE: The names of the compounds have been modified so they are self-consistent throughout the text.

- It will be better to see a scheme for the synthesis of the compounds in the paper.

AUTHORS' RESPONSE: As requested a scheme, Scheme 1, was added.

- What do the authors mean by saying SG of Cys25 or SG-Te?

AUTHORS' RESPONSE: The authors have followed the literature norm in discussing the protein-substrate interactions:

https://www.ebi.ac.uk/pdbe-srv/pdbechem/atom/show?cid=CYS&name=SG

PDBeChem : Atom of Molecule

Molecule : CYS Atom : SG

Atom of a chemical element, that composes a molecule

Atom Name SG

Element Symbol S

PDB Name SG

To enhance understanding, an explanatory comment has been added.

- In Page 22, line 2, the reference number was not mentioned.

AUTHORS' RESPONSE: The missing reference has been added

- The graphical abstract does not provide any information about the structures of the compounds. The authors can make another more informative one.

AUTHORS' RESPONSE: A new GrAb has been generated giving the structure of the studied molecules

- In highlights, it is mentioned that "Some compounds are known to effectively inhibit cathepsin S", however, according to the provided constants, compound 3 seems not to be so effective. It is better to change this sentence.

AUTHORS' RESPONSE: The Highlights has been modified as suggested

Reviewer #2: MOLSTRUC-D-21-01523

The authors have studied "Crystal structures and docking (cathepsin S) studies on bioactive trichloridotellurium(IV) 4-oxo-2,4-diphenylbutan-1-ides". My opinion is that the manuscript is interesting, and finally, the topic is of interest to the readership of this journal. Therefore, I recommend publication of this work after minor revision as follows:

1. This is work is good, however, it is a paper about docking studies. Grammar corrections should be made on the entire manuscript.

AUTHORS' RESPONSE: the entire modified manuscript was subjected to an English language spelling and grammar check

2. Full analytical data must be provided for novel compounds, including HRMS/elemental analysis.

AUTHORS' RESPONSE: The elemental analysis data are included in the manuscript. However, HTMS data were not recorded for these compounds.

3. 1H NMR, 13C NMR and IR figures have not been reported in this study which should be included.

AUTHORS' RESPONSE: The full details of the IR, ^{1}H and $^{13}C\{^{1}H\}$ NMR data are included in the manuscript. The spectroscopic data were extracted from a Ph.D. thesis dating back to 2005 and, regrettably, the original spectra were not included in the thesis and are no longer available. Further, the samples are no longer available.

4. The authors studied only structure and docking studies and limited explanation given. So need to may be rewrite and added more physical properties oriented studies.

AUTHORS' RESPONSE: The study was prompted by the variable biological activity of organotellurium three derivatives. Herein, full characterisation of these derivatives is provided, including by X-ray crystallography, and the docking study was performed to rationalise the published experimental data, data which is also in included in the manuscript.

5. Biologically related added some other studies.

AUTHORS' RESPONSE: As above for point 4. The biology has already been published.

6. What is the melting point of the crystals?

AUTHORS' RESPONSE: The melting points were determined on ground samples in capillaries. This additional information is now included.

7. Give the probability percentage in crystal structure Figures.

AUTHORS' RESPONSE: The percentages are given in the caption to Figure 3.

8. The molecular packing structures and unit cells are missing. Why?

AUTHORS' RESPONSE: The unit-cell outlines are given in the relevant images of Figures 5, 6 and 7

9. The authors not mentioned about the π-π stacking interactions, why?

AUTHORS' RESPONSE: When present, the π…π interactions are mentioned in the descriptions of the molecular packing

10. Authors should check all of the references again in the present form.

All references have been confirmed

Crystal structures and docking studies in cathepsin S of bioactive 1,3-diphenyl-4-(trichloro-λ^4-tellanyl)but-2-en-1-one derivatives

Stella Hernandes Maganhi[1,2§], Ignez Caracelli[1*], Julio Zukerman-Schpector[2], Rodrigo L. O. R. Cunha[3], Mauricio Angel Veja-Teijido[2†], Edward R.T. Tiekink[4*]

[1] BioMat, Departamento de Física, Universidade Federal de São Carlos, 13565-905 São Carlos, SP, Brazil. orcid.org/0000-0003-4945-7485

[2] Departamento de Química, Universidade Federal de São Carlos, 13565-905 São Carlos, SP, Brazil. orcid.org/ 0000-0003-2191-4074

[3] Centro de Ciências Naturais e Humanas, Universidade Federal do ABC, 09210-170, Santo André, SP, Brazil

[4] Research Centre for Crystalline Materials, School of Medical and Life Science, Sunway University, 47500 Bandar Sunway, Selangor Darul Ehsan, Malaysia. orcid.org/0000-0003-1401-1520

* Corresponding authors: Ignez Caracelli, BioMat, Departamento de Física, Universidade Federal de São Carlos, 13565-905 São Carlos, SP, Brazil; E-mail: ignez@df.ufscar.br; Tel. no.: +55 16 33519741. Edward R.T. Tiekink, Research Centre for Crystalline Materials, School of Medical and Life Science, Sunway University, 47500 Bandar Sunway, Selangor Darul Ehsan, Malaysia; E-mail: edwardt@sunway.edu.my

§ Present address: Universidade do Estado de Minas Gerais - Unidade Ituiutaba, 38302-192 Ituiutaba, MG, Brazil

†Present address: Computational Chemistry and Biology Group,CCBG, DETEMA, Facultad de Química-Universidad de la República, CC1157 Montevideo, Uruguay

Abstract

The molecular structures of three 1,3-diphenyl-4-(trichloro-λ^4-tellanyl)but-2-en-1-one derivatives (**1**–**3**), show similar coordination geometries defined by methylene-C, three chloride and carbonyl-O atoms. In each case, the resulting CCl_3O donor set defines a square-pyramid with the vacant space opposite the methylene-C atom occupied by a lone-pair of electrons. Each of the molecules dimerises in the crystal via weak intermolecular Te···Cl interactions so a distorted ψ-pentagonal-bipyramidal geometry ensues. Previous work has shown these compounds to inhibit cathepsin S to varying extents, with **2**, having 2-methoxy substituents in the 2-position of rings, being particularly effective. Molecular docking calculations of cathepsin S with ligands **1'**–**3'** (i.e. cations derived from **1**–**3** by removal of one of the tellurium-bound chloride atoms) showed the higher experimental second order inactivation rate of **2**, compared with the other two ligands, is explained by the observation that the ligand occludes the entrance to the channel thereby blocking access to the catalytic Cys25 site and also because **2'** occupies part of the crucial subsite S3 of the protein.

Keywords

Tellurium(IV); crystal structure; molecular packing; molecular docking; cathepsin S

1. Introduction

While tellurium compounds have yet to make the pharmacopeia [1, 2], there is growing interest in evaluating tellurium(IV) compounds, including organotellurium(IV) derivatives, for biological activity against a broad range of disease [3-11]. By far the most prominent tellurium compound in this context is a salt, namely salt ammonium trichloride (dioxyethylene-O,O')tellurate, known as AS-101, and illustrated in Fig. 1a [12]. A broad range of biological potential is known for AS-101 as this salt has been demonstrated to inhibit angiogenesis [13], is a potent immunomodulator [14], is effective against psoriasis [15] and human papillomavirus [16], can be used in the prevention of infertility suffered by chemotherapy patients [17] and in preventing and reversing type-1 diabetes [18]. Complementing experimental studies and crucial for drug development is an understanding of the molecular mechanism(s) of action.

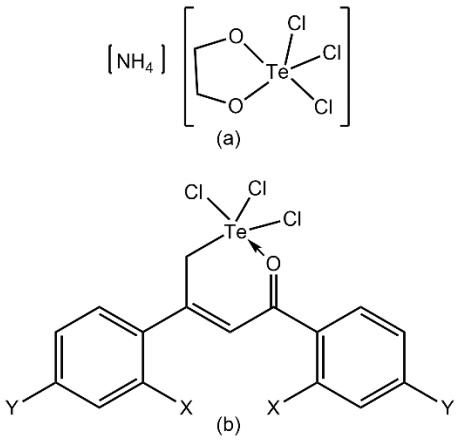

Fig. 1: Chemical diagrams of (a) ammonium trichlorido(dioxoethylene-O,O')tellurate (AS-101) and (b) 1,3-diphenyl-4-(trichloro-λ^4-tellanyl)but-2-en-1-one (**1**), i.e. with X = Y = H. Compound **2** has X = OMe and Y = H; and **3**, X = H and Y = OMe.

In this context, research on relatively non-toxic AS-101 reveals the trichlorido(dioxoethylene-O,O')tellurate anion to be a specific inhibitor of cysteine proteases such as papain and cathepsin B, by forming a covalent Te–S bond with the thiolate-S atom of the Cys29 residue [14]. Allied research has been conducted on tellurium-based compounds targeting this class of enzyme, including several series of organotellurium compounds, some of which that exhibited greater irreversible inhibitory activity than AS-101 against cathepsin B while at the same being irreversible inhibitors of cathepsins K, L and S [19-21]. In a comprehensive study of a number of hypervalent tellurium/organotellurium(IV) compounds, one particular series, i.e. **1**–**3** in Fig. 1b, was evaluated for inhibitory activity against cathepsins B, K, L and S. Remarkably, **2** exhibited significantly greater inhibition of cathepsin S compared to cathepsins B, K and L and in relation to the other derivatives [21]. The variety in cathepsin inhibition values exhibited by a particular compound relates to the interaction of its metabolite with the various subsites in the enzyme, sites which are responsible for the specific action of the protease [22, 23]; the nature of the different subsites in cathepsins B, K, L and S were detailed in a recent study [24].

It is well established that targeting all of the above-mentioned cathepsins, i.e. B, K, L and S, offers hope in curing many types of disease [25], for example, inhibiting each combats metastasis in different types of cancer [26-30]. In addition, specific cathepsins relate to specific pathological disorders. For example, the inhibition of cathepsin K is known to promote bone regeneration and to alleviate the symptoms associated with osteoporosis [31, 32]; it is noted that inhibition of cathepsin K has proven elusive [33]. Of particular relevance to the present study is the role of cathepsin S in human disease.

An example of cathepsin S (Enzyme code (EC): 3.4.22.27) is illustrated in Fig. 2, i.e. PDB [34] code 1MS6 [35]. Cathepsin S is known to act as an endopeptidase, facilitating the breaking of non-terminal peptide bonds [36]. Cathepsin S comprises one polypeptide chain

comprising 217 amino acid residues and has a molecular mass of approximately 24 kDa [37]. In the chain, there are nine cysteine residues, with six of them part of a disulphide bond (Cys22–Cys66, Cys56–Cys99 and Cys158–Cys206) while the other three are isolated (Cys2, Cys25, Cys110) [37]. The active site of cathepsin S is characterised by a catalytic triad comprising Cys25, His164 and Asn184 residues [32, 33]. The subsites S1, S1′, S2 and S3 [38] are arranged along the catalytic cleft, with the amino acids as specified recently [24].

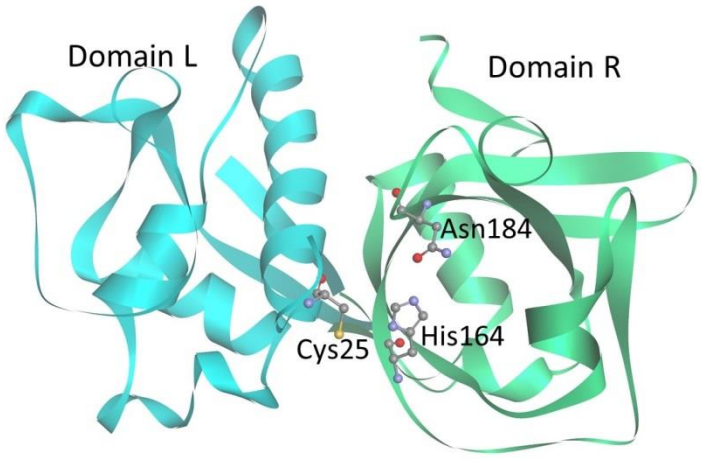

Fig. 2: Cathepsin S secondary structure illustrated for PDB code 1MS6 [35] showing the Cys25 residue in the active site. The L domain features three alpha helices in the secondary structure, while the R domain features anti-parallel beta-strands. The catalytic site includes amino acids Cys25, His164 and Asn184.

Cathepsin S is distinguished from many other cathepsins in that it remains catalytically active under neutral pH conditions, having optimal activity in the pH range 6.0–7.5, in contrast to other cathepsins which exhibit greater activity under acidic conditions [39]. This has the important consequence that cathepsin S remains stable in lysosomes and can exert physiological roles outside that environment. In response to inflammatory mediators, e.g. pro-inflammatory cytokines and neutrophils, macrophages and microglia secrete cathepsin S [39, 40].

The key step in the inhibition of any cysteine protease by a tellurium compound ("tellurium ligand") is the loss of a negatively charged tellurium-bound labile group, often a halide, and the concomitant formation of a covalent Te–S bond with a cysteine reside [41, 42]. Effective inhibition will see optimal interactions of the tellurium ligand with the various subsites of the specific cathepsin under investigation [22, 23]. As a continuation of investigations into the modes of association of putative tellurium-based drugs with a variety of cathepsins [43, 44], herein a docking study of three previously described [21, 45] 1,3-diphenyl-4-(trichloro-λ^4-tellanyl)but-2-en-1-one derivatives (**1**–**3**), Fig. 1b, with cathepsin S is reported. Compounds **1**–**3** showed variable inhibition values against this protease with **2** being particularly effective. The specific aim of the present study is to rationalise the differential inhibition behaviour of **1**–**3**. As the crystal structures of **1**–**3** are not known, these were determined and also described herein.

2. Experimental

2.1 Synthesis and crystal growth

Compounds **1**–**3** were prepared as shown in Scheme 1 following previously described procedures [21, 45, 46]. Briefly, tellurium tetrachloride (2.72 g, 10 mmol) reacted with 10 mmol of the appropriate acetophenone (**1**), 2-methoxyacetophenone (**2**) and 4-methoxyacetophenone (**3**) in 25 mL of dry chloroform. The obtained suspension was stirred under reflux for 30 minutes, after this another equivalent (10 mmol) of the acetophenone was added to the solution and it was refluxed for 12 h. Then, the reaction mixture was cooled to room temperature, concentrated and crystals of **1-3** were obtained from the slow evaporation from the slow evaporation of the respective chloroform solutions layered with petroleum ether. The reported melting points are for the ground samples.

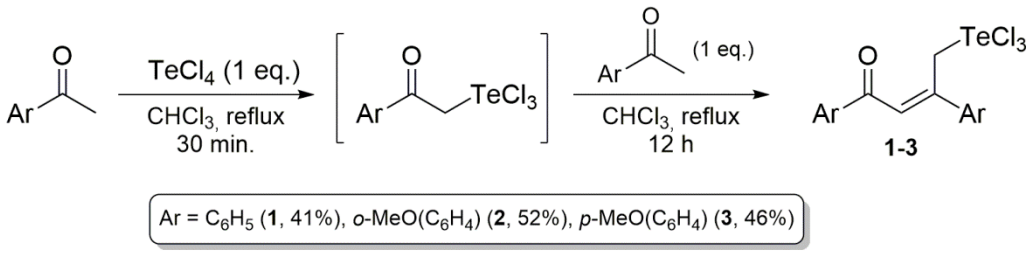

Scheme 1. Synthesis of the compounds described in the paper

(Z)-1,3-diphenyl-4-(trichloro-λ^4-telluro)-but-2-en-1-one (**1**). Green crystals (1.91 g, 42% yield), m.p. 138-139 ºC (dec.). ^{1}H NMR (500 MHz, $CDCl_3$) δ 8.16 (dd, ^3J 8.5, ^4J 1.2, 2H), 7.77-7.73 (m, 1H), 7.69-7.67 (m, 2H), 7.60-7.52 (m, 5H), 7.42 (s, 1H), 5.17 (s, 2H). ^{13}C NMR (125 MHz, $CDCl_3$, ppm) δ 196.4, 158.5, 140.4, 136.2, 135.5, 131.6, 130.1, 129.42, 129.37, 127.6, 120.1, 135.4, 62.6. ^{125}Te NMR (157.98 MHz, dmso-d^6, referenced to PhTeTePh at 422 ppm) 1516.2. IR (KBr) 2910, 1977, 1911, 1732, 1593, 1564, 1471, 1427, 1377, 1298, 1232, 1059, 1001, 864, 756, 677, 662, 561, 509. Anal. calc. for $C_{16}H_{13}Cl_3OTe$: C, 42.21; H, 2.88, found C, 42.47; H, 2.58.

(Z)-1,3-bis(2-methoxy-phenyl)-4-(trichloro-λ^4-telluro)-but-2-en-1-one (**2**). Red crystals (2.68 g, 52% yield), m.p. 192-195 °C (dec.). ^{1}H NMR (500 MHz, $CDCl_3$) δ 7.93 (dd, ^3J 7.9, ^4J 1.8, 1H), 7.65-7.61 (m, 1H), 7.47-7.43 (m, 2H), 7.41 (s, 1H), 7.09-7.03 (m, 2H), 7.01 (d, ^3J 8.4, 1H), 6.97 (d, ^3J 8.2, 1H), 5.22 (s, 2H), 3.92 (s, 3H), 3.91 (s, 3H). ^{13}C (125 MHz,$CDCl_3$, ppm) δ 197.2, 160.7, 157.4, 156.1, 137.5, 133.1, 132.4, 130.4, 128.6, 127.5, 126.0, 121.6, 121.5, 112.5, 111.7, 63.4, 56.4, 55.9. ^{125}Te (157.98 MHz, dmso-d^6, referenced to PhTeTePh at 422 ppm) 1357.9. IR (KBr) 3011, 2937, 2837, 1579, 1485, 1464, 1443, 1364, 1282, 1240, 1169, 1124, 1024, 885, 777, 756, 640, 503, 451. Anal. calc. for $C_{18}H_{17}Cl_3O_3Te$: C, 41.96; H, 3.33, found C, 41.88; H, 3.31.

(Z)-1,3-bis(4-methoxy-phenyl)-4-(trichloro-λ^4-telluro)-but-2-en-1-one (**3**). Red crystals (2.37 g, 46% yield), m.p. 182-183 °C (dec.). ^{1}H NMR (300 MHz,$CDCl_3$) δ 8.17 (d, ^3J 9.3, 2H),

7.65 (d, ^{3}J 9.0, 2H), 7.32 (s, 1H), 7.03 (d, ^{3}J 9.3, 2H), 7.02 (d, ^{3}J 9.0, 2H), 5.10 (s, 2H), 3.95 (s, 3H), 3.89 (s, 3H). ^{13}C NMR (75 MHz, $CDCl_3$) δ 193.4, 162.7, 152.3, 130.4, 128.0, 126.6, 124.9, 119.6, 114.2, 113.9, 113.8, 55.4, 55.2, 55.1, 55.0. ^{125}Te NMR (157.98 MHz, dmso-d^6, referenced to PhTeTePh at 422 ppm) 1359.4. IR (KBr) 3097, 2931, 2837, 2050, 1593, 1542, 1479, 1421, 1356, 1319, 1261, 1169, 1016, 914, 900, 827, 637, 509. Anal. calc. for $C_{18}H_{17}Cl_3O_3Te$: C, 41.96, H, 3.33, found C, 41.93, H, 3.32.

2.2 Crystal structure determination

Intensity data for **1**–**3** were measured at room temperature on an Enraf Nonius TurboCAD4 diffractometer using graphite-monochromatized MoKα radiation (λ = 0.71073 Å). The absorption corrections were applied using the ψ-scan method in CAD4 Express [47], and data processing was accomplished using XCAD4 [48]. Unit-cell data, X-ray data collection parameters and details of the structure refinement are summarised in Table 1. The structures were solved by direct methods using SIR92 [49] and full-matrix least-squares refinement on F^2 followed (anisotropic displacement parameters and C-bound H atoms in their idealised positions) [50]. A weighting scheme of the form $w = 1/[\sigma^2(Fo^2) + (aP)^2 + bP]$ where $P = (Fo^2 + 2Fc^2)/3$ was introduced in each case. The residual electron density peaks listed in Table 1 for **2** are 1.01 and 1.32 Å from the tellurium atom. Similarly, those indicated for **3** are 0.95 and 1.10 Å from the heavy atom. The programs WinGX [51], PLATON [52], ORTEP-3 for Windows [51] and DIAMOND [53] were also used in the analysis.

Table 1

Crystallographic data and refinement details for **1**–**3**.

	1	**2**	**3**
Formula	$C_{16}H_{13}Cl_3OTe$	$C_{18}H_{17}Cl_3O_3Te$	$C_{18}H_{17}Cl_3O_3Te$
Formula weight	455.21	515.27	515.27

Crystal colour, habit	Irregular, green	Irregular, red	Irregular, red
Crystal size/mm	0.10 × 0.20 × 0.20	0.10 × 0.12 × 0.18	0.08 × 0.12 × 0.18
Crystal system	triclinic	triclinic	triclinic
Space group	$P\bar{1}$	$P\bar{1}$	$P\bar{1}$
a/Å	8.9308(7)	7.3665(9)	9.6177(9)
b/Å	9.6253(9)	10.371(1)	10.546(1)
c/Å	10.986(1)	13.321(1)	11.387(1)
α/°	77.065(7)	84.594(9)	104.713(8)
β/°	86.827(10)	76.224(10)	113.291(9)
γ/°	63.089(13)	77.036(8)	100.748(9)
V/Å^3	819.59(15)	962.33(17)	971.07(17)
Z/*Z′*	2/1	2/1	2/1
D_c/g cm^{-3}	1.845	1.778	1.762
F(000)	440	504	504
λ(Mo*K*α)/mm^{-1}	2.298	1.976	1.958
Measured data	4821	3753	3834
θ range/°	2.4 – 30.0	1.6 – 25.5	2.1 – 25.5
Unique data	4553	3585	3601
R_{int}	0.027	0.077	0.061
Observed data ($I \geq 2.0\sigma(I)$)		3416	2629 2817
R, obs. data; all data	0.034; 0.085	0.051; 0.124	0.061; 0.158
a, *b* in weighting scheme	0.047, 0.330	0.088, 0	0.128, 0
R_w, obs. data; all data	0.065; 0.097	0.080; 0.137	0.080; 0.171
$\Delta\rho_{max,\ min}$/e Å^{-3}	0.55, -0.66	1.57, -1.28	2.83, -1.78
CSD deposition no.	2074123	2074124	2074125

2.3 Generation of ligand structures for the docking studies

The experimentally determined structures of **1**–**3** were used as the starting points for generating the ligand structures for the docking studies. Each of the structures was made mono-cationic by the removal of a tellurium-bound chloride anion. As there are three different chlorides about the tellurium atom in **1**–**3**, three different ligand structures were generated for each compound and used as the input into the docking calculations.

2.4 Docking studies

In the present investigation , the GOLD 5.0.1 program [54, 55] was used with the GoldScore fitness function which allows for a variety of factors, e.g. the energies due to hydrogen bonding and van der Waals interactions, and ligand torsion strain. The performed calculations were based on the formation of a covalent complex, via a Te–S bond, involving the Cys25 residue of the catalytic site of cathepsin S and the tellurium atom of the different tellurium ligands. The constraint parameter of the GOLD program was employed to establish a range for the Te–S bond length, i.e. 2.4 to 3.5 Å, and in all cases the docking simulations were preformed assuming a rigid enzyme. For the tellurium ligands, two different calculations were performed due to the fact that the X-ray crystal structures of **1**–**3** showed the presence of an intramolecular Te···O(carbonyl) interaction giving rise to a "closed" conformation through a pseudo six-membered chelate ring (see below), so, at first, the Te···O(carbonyl) separation was restrained to the crystallographic value in each case and the rest of the molecule allowed flexibility. Further calculations were also performed releasing the Te···O(carbonyl) distance restraint which gave rise to an "open" conformation where the Te···O(carbonyl) interaction was not present. Only amino acid residues within a radius of 10.0 Å around the ligand cavity were considered. All water molecules were removed since there are none in the active site of cathepsin S and are therefore, not influential in the interactions.

For molecular visualisation of the poses and for the analysis of interactions and alignments, the DS Visualizer program 3.5 [56] was employed.

3. Results and discussion

3.1 Experimental molecular structures

The experimental molecular structures of **1**–**3** are shown in Fig. 3 and selected geometric parameters are listed in Table 2. The tellurium(IV) centre in **1** is coordinated by three chloride anions, the methylene-carbon atom of the mono-anionic 4-oxo-2,4-diphenylbutan-1-ide ligand with the five-coordinate geometry being completed by the carbonyl-oxygen atom. The mode of coordination of the organic ligand leads to the formation of six-membered $TeOC_4$ chelate ring which is non-planar. The best description for the conformation of the chelate ring is a half-chair with the tellurium atom lying 0.889(6) Å above the plane defined by the five remaining atoms which are close to co-planar with a r.m.s. deviation = 0.035 Å. The C5–C10 phenyl ring forms a dihedral angle 9.7(3)° with the planar part of the chelate ring and the comparable angle for the C11-C16 ring is 3.9(3)°; the dihedral angle between the outer rings is 13.3(3)°, indicated a folded conformation. The coordination geometry for the tellurium atom is based on a square pyramid based on the value of τ = 0.06, which compares with the τ values of 0.00 and 1.00 for ideal square-pyramidal and trigonal-pyramidal geometries, respectively [57]. In this description, the tellurium atom lies 0.1236(7) Å out of the plane (r.m.s. deviation = 0.068 Å) in the direction opposite to the methylene-C1 atom which occupies the apical position. The unoccupied region about the tellurium(IV) centre is presumably occupied by a stereochemically-active lone-pair of electrons. When intermolecular Te···Cl interactions are considered (see below) the coordination geometry is best described as being distorted ψ-pentagonal-bipyramidal. While the bond lengths associated with the mutually trans-disposed Cl1 and Cl3 atoms differ by less than 0.02 Å, the Te–Cl2 bond length of 2.4254(10) Å, with the Cl2 atom trans to the carbonyl-O1 atom, is systematically shorter than the Te–Cl1, Cl3 bonds, Table 2, reflecting the relative weak nature of the Te···O1, formally dative bond.

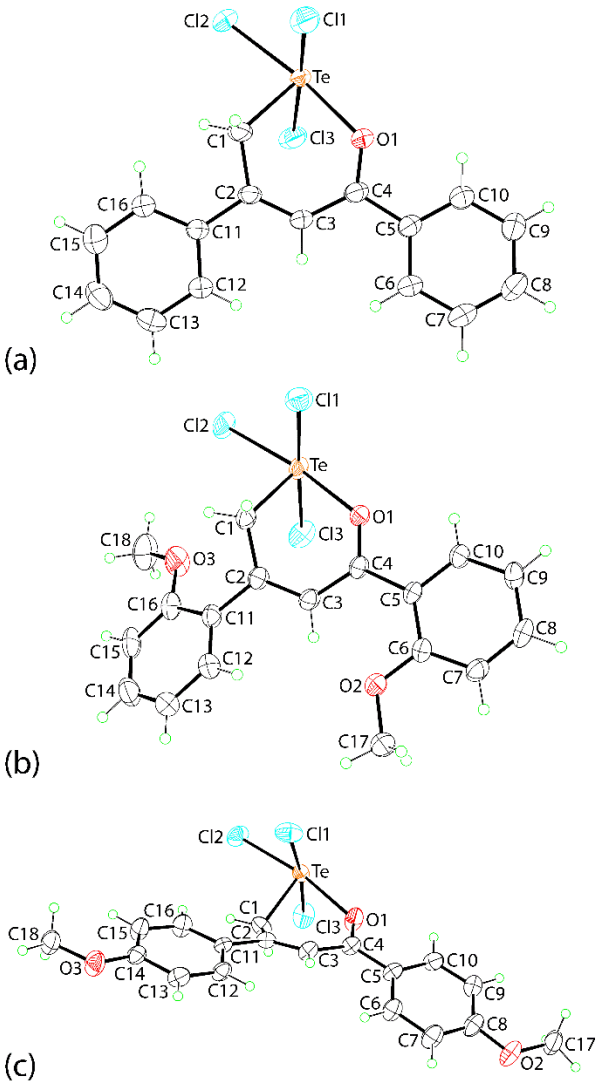

Fig. 3. Molecular structures of **1**–**3**, showing atom labelling and displacement ellipsoids at the 35% probability level.

Table 2

Summary of key geometric parameters (Å, º) for **1**–**3**.[a]

Parameter	**1**; n = 3	**2**; n = 1	**3**; n = 2
Te–C11	2.4826(13)	2.502(2)	2.461(2)
Te–C12	2.4254(10)	2.4240(15)	2.4025(19)
Te–C13	2.5004(12)	2.479(2)	2.520(2)
Te–O1	2.241(3)	2.287(4)	2.292(5)
Te–C1	2.116(4)	2.116(6)	2.102(7)
Te–Cl(n)[i]	3.8738(12)	3.742(2)	4.014(3)

Cl1–Te–Cl2	89.72(4)	91.77(7)	88.51(8)
Cl1–Te–Cl3	173.82(4)	175.65(6)	173.16(7)
Cl2–Te–Cl3	92.34(4)	92.23(7)	88.43(8)
Cl1–Te–C1	87.39(14)	86.58(18)	88.5(2)
Cl3–Te–C1	86.84(14)	91.65(18)	85.5(2)
Cl2–Te–O1	170.32(8)	167.59(12)	169.80(15)
O1–Te–C1	82.29(14)	77.36(18)	77.8(2)

a Symmetry operation i: **1** 1-x, -y, 2-z; **2** 1-x, -y, 2-z; **3** 1-x, 1-y, -z.

A quite similar coordination geometry to that just described or **1** is found for the tellurium(IV) centre in **2**, Fig. 3b. In the chelate ring, the tellurium atom lies 1.177(8) Å above the plane defined by the remaining atoms (r.m.s. deviation = 0.076 Å); the outer C5- and C11-rings of the organic ligand form dihedral angles of 14.8(2) and 39.97(18)°, the planar region of the chelate ring indicating a more twisted conformation for the ligand; the angle between the phenyl rings is 25.91(16)°. The tellurium atom lies 1.969(6) Å out the basal plane defined by Cl_3O atoms (r.m.s. deviation = 0.103 Å), again away from the methylene-C1 atom. The systematic variations in the Te–Cl bond lengths prevail, Table 2. The chemical difference between **1** and **2** rests with the presence of two methoxy substituents in the latter. As seen from Fig. 3b, the methyl group of the O2-methoxy substituent occupies the bay region defined by the 4-oxo-2,4-diphenylbutan-1-ide ligand, consistent with the deformation in this ligand in **2** compared with **1**. The O3-methoxy substituent is orientated so that the O3-atom is directed towards the tellurium atom but the Te···O3 separation of 3.946(5) Å is too long to be considered a significant bonding interaction. Rather, this is more likely a reflection of a significant intramolecular methylene-C1-H···O3 interaction with H···O3 = 2.19 Å. This assessment is vindicated in the value τ, i.e. 0.13, indicating a small deviation from a regular square-pyramidal geometry. The tellurium atom lies 0.1314(13) Å

out of the Cl_3O plane (r.m.s. deviation = 0.103 Å), again in the direction away from the C1 atom.

The third structure, **3**, illustrated in Fig. 3c, exhibits some deviations from **1** and **2**. The half-chair conformation of the chelate ring sees the tellurium atom lying 1.06(10) Å out of the C_4O plane (r.m.s. deviation = 0.120 Å), being intermediate in its deviation cf. **1** and **2**. The dihedral angles between the constituent C_4O atoms of the chelate ring and the C5- and C11-phenyl rings are 29.4(3) and 16.3(3)°, respectively; the dihedral angle between the phenyl rings is 19.1(4)°, again intermediate between the angles found in **1** and **2**. In **3**, the 4-oxo-2,4-diphenylbutan-1-ide ligand is directed away from the Cl3 atom, whereas the opposite in true in **1** and **2**. The calculated value of τ is 0.06 [56], indicating a coordination geometry close to square-pyramidal with the tellurium atom lying 0.1732(17) Å out of the Cl_3O plane (r.m.s. deviation = 0.035 Å) in the opposite direction to the C1 atom, as for **1** and **2**. An overlay diagram, shown in Fig. 4, highlights the different molecular conformations found in **1**–**3**.

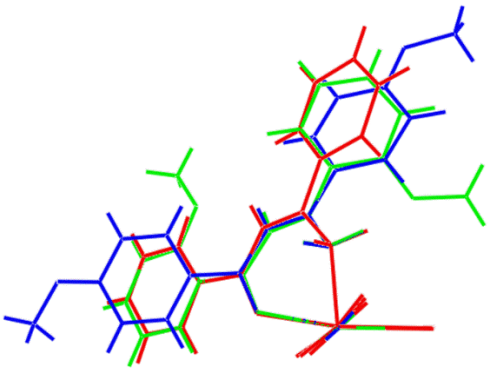

Fig. 4: Overlay diagram of **1** (red image), **2** (green) and inverted-**3** (blue) with the molecules superimposed so that the Te, O1 and C1 atoms are coincident.

The most closely related literature structure to **1**–**3** is the compound with the phenyl/substituted-phenyl rings replaced by methyl substituents [58]. As would be

anticipated, the molecular structure of Te[CC(Me)=C(H)C(=O)Me]Cl_3 displays much the same geometric and conformational features as described above.

3.2 Molecular packing

The key feature of the molecular packing of each of **1**–**3**, is the presence of secondary Te···Cl interactions [59-61], which occur about a centre of inversion in each of the crystals, so that centrosymmetric dimers are formed. The mode of association between the dimeric aggregates differs in each case, however. A listing of the most prominent points of contact between the dimers in **1**–**3** is given in Table 3.

In the crystal of **1**, the centrosymmetric supramolecular dimer, Fig. 5a, is sustained by Te···Cl3^{i} interactions of 3.8738(12) Å which are marginally longer than the sum of the van der Waals radii [62] of 3.81 Å, emphasising their weak nature; symmetry operation i: 1-x, -y, 2-z. The only contacts occurring at distances less than the sum of the respective van der Waals radii [52, 63] are phenyl-C–H···Cl interactions, involving each of the chloride atoms. These interactions stabilise supramolecular layers as shown in Fig. 5b that stack along the a-axis, Fig. 5c. The closest inter-layer interactions occur between centrosymmetrically-related C11-phenyl rings with rather long inter-centroid separations of 4.541(3) Å symmetry operation: -x, 1-y, 1-z. However, the rings are significantly off-set from each other with the distance between parallel rings being 3.597(2) Å and closest C···C contact of 3.629(9) Å consistent with an edge-to-edge interaction between the rings.

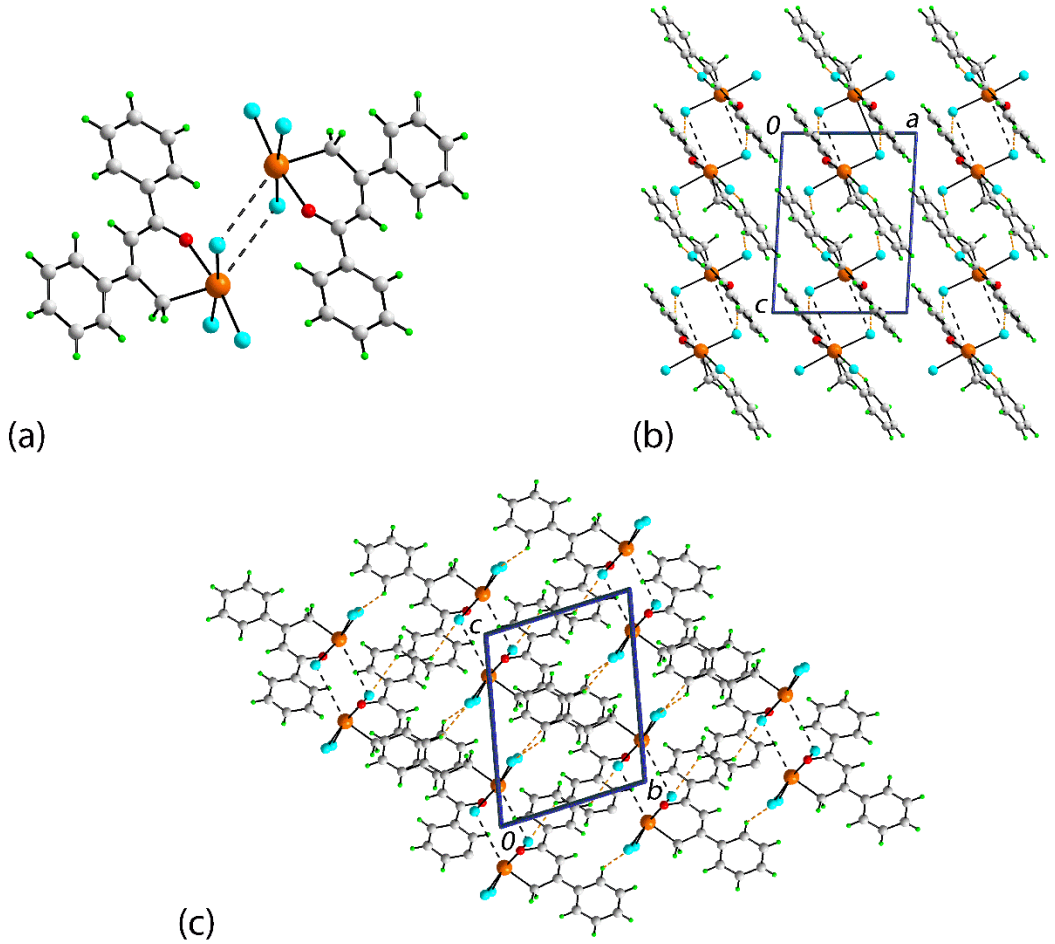

Fig. 5. Molecular packing in **1**: (a) supramolecular dimer mediated by weak Te···Cl bonding interactions (black dashed lines), (b) layer in the bc-plane mediated by C–H···Cl interactions shown as orange dashed lines and (c) view of the unit cell contents in projection down the b-axis.

In **2**, the centrosymmetric dimer involves bridging $Cl1^{i}$ atoms with the intermolecular distance being 3.742(2) Å, i.e. a little less than the sum of the van der Waals radii; symmetry operation i: 1-x, -y, 2-z, Fig. 6a Thus, the presence of additional methyl-C–H···Cl and π···π interactions contribute to the three-dimensional architecture in the crystal of **2**, Table 3. The combination of C17–H···Cl1 with π(C5–C10)···π$(C5–C10)^{ii}$ contacts between centrosymmetrically related rings (inter-centroid distance = 3.530(4) Å for symmetry operation ii: -x, 1-y, 2-z) gives rise to supramolecular layers in the ab-plane, Fig. 6b. The layers stack along the c-axis and the protruding phenyl-C11-C16 rings inter-digitate via

π(C11–C16)···π(C11–C16)^{iii} contacts with an inter-centroid separation of 3.604(5) Å (symmetry operation iii: 1-x, 1-y, 1-z), Fig. 6c.

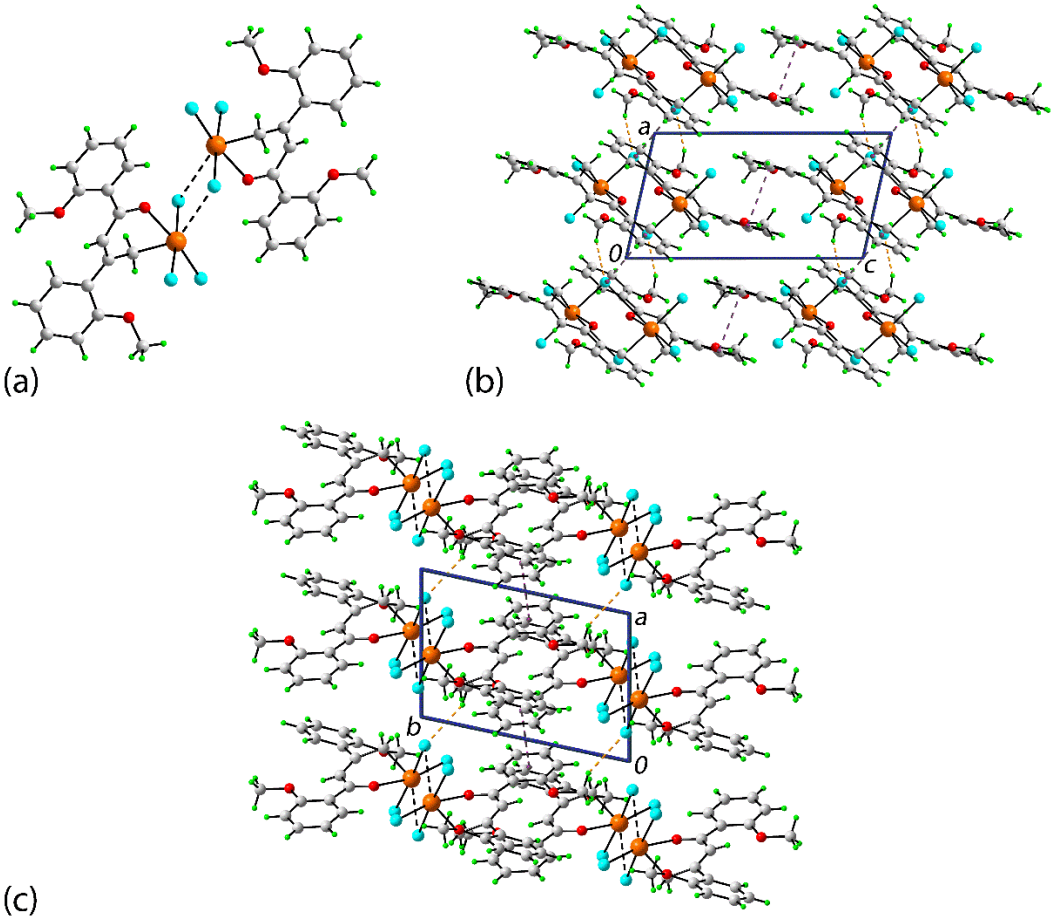

Fig. 6. Molecular packing in **2**: (a) supramolecular dimer mediated by Te···Cl bonding interactions (black dashed lines), (b) layer in the ab-plane mediated by C–H···Cl and π···π stacking interactions shown as orange and purple dashed lines, respectively, and (c) view of the unit cell contents in projection down the b-axis.

The centrosymmetric dimer about the {···Te–Cl}$_2$ synthon formed in **3** involves the Cl2 atom, i.e. the atom trans to the carbonyl-O1 atom and forming the shorter of the Te–Cl bonds in **1**–**3**, Fig. 7a. Therefore, and as seen from Table 3, each dimer formed in molecular packing of **1**–**3** involves the participation of a different chloride atom. Supramolecular layers

are formed in the crystal of **3**, arising from the combination of phenyl-C12–H···Cl2 along with methyl-C–H···π(C5-phenyl, C11-phenyl) interactions, Table 3. Layers lie parallel to the bc-plane, Fig. 5b. The most notable interactions between layers which inter-digitate along the a-axis, Fig. 5c, appear to be very weak methyl-C17–H···Cl2, Cl3.

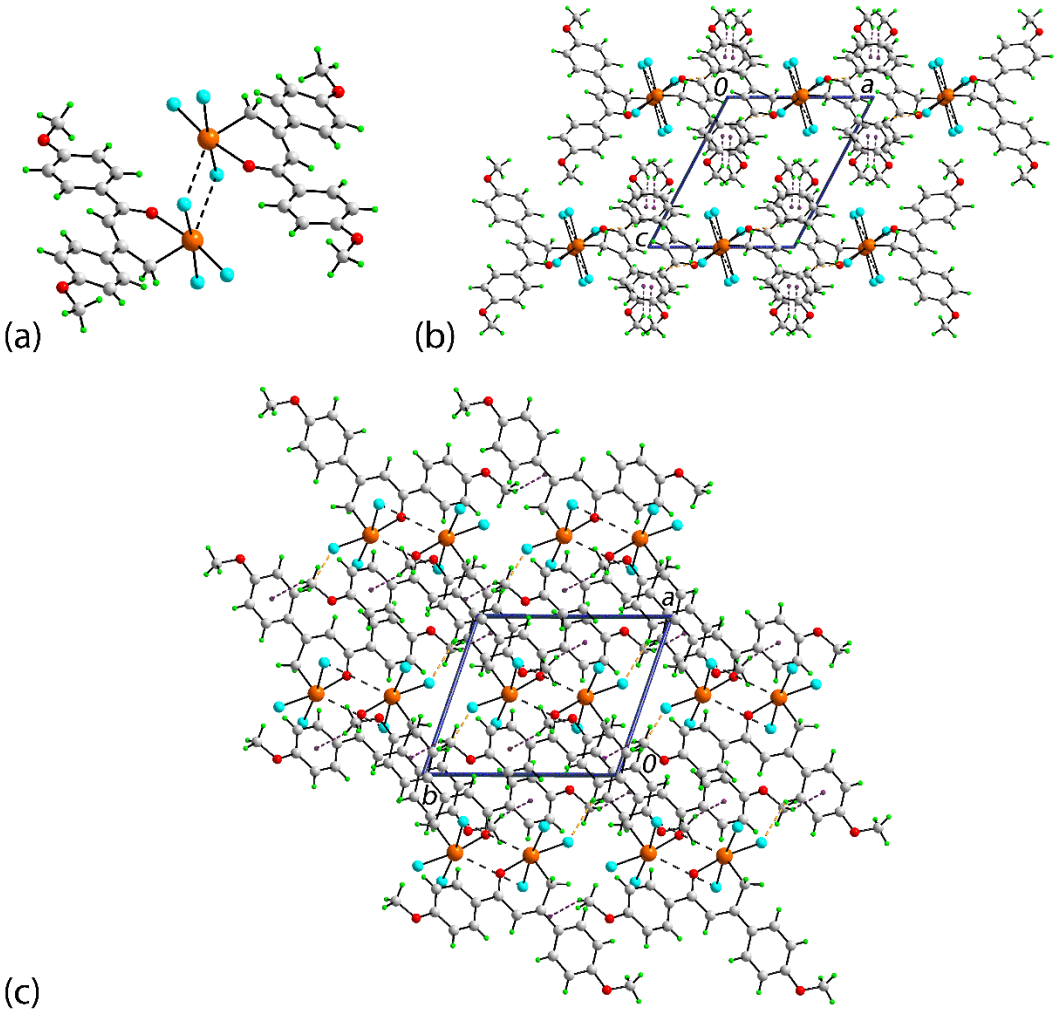

Fig. 7. Molecular packing in **3**: (a) supramolecular dimer mediated by Te···Cl bonding interactions (black dashed lines), (b) layer in the ab-plane mediated by C–H···Cl and C–H···π interactions shown as orange and purple dashed lines, respectively, and (c) view of the unit cell contents in projection down the b-axis.

Table 3

Summary of the intermolecular interactions (Å, º) in the crystals of **1**–**3**.

1							
C7	H7	Cl3	0.93	2.91	3.661(6)	139	1-x, 1-y, 2-z
C12	H12	Cl2	0.93	2.89	3.669(5)	142	x, 1+y, z
C16	H16	Cl1	0.93	2.84	3.668(5)	150	1-x, -y, 1-z
2							
C17	H17A	Cl1	0.96	2.76	3.602(9)	147	-1+x, 1+y, z
3							
C12	H12	Cl2	0.93	2.81	3.578(9)	141	-1+x, y, z
C17	H17c	Cg(C11–C16)		0.96	2.89	3.783(10)	156 -x, 1-y, -z
C18	H18c	Cg(C5–C10)	0.96	2.83	3.735(9)	158	-x, -y, -z
C17	H17a	Cl2	0.96	2.93	3.768(11)	146	-x, -y, -1-z
C17	H17b	Cl3	0.96	3.06	3.989(9)	102	-1+x, -1+y, -1+z

3.3 Docking studies

The protein-ligand complex structure used in the present study was the one with pdb code 1MS6 [35], i.e. cathepsin S in its complex with (2S)-N-[2(benzyloxy)-1-cyanoethyl]-4-methyl-2-[(morpholine-4-carbonyl)amino]pentanamide with pdb code BLN. As experimental data showed there is a covalent bond formation between the tellurium atom and the SG of Cys25 [19, 21], docking calculations were conducted with the SG–Te bond length restricted to be within the interval 2.4 to 3.5 Å; SG refers to the thiolate-S atom of Cys25.

As already mentioned in 2.4, calculations were performed with the Te···O(carbonyl) bond fixed at the crystallographic value, representing the closed conformation, and then with this restraint released so the ligand was fully flexible. In order to enable the formation of the SG–Te bond, each of the three chloride atoms was removed in turn, in order to assess which mono-cationic structure gave rise to the most efficient SG–Te interaction. A summary of the docking results is shown in Table 4 where it can be seen that

the species forming the shortest SG–Te distances in each category, that is in both closed and open conformations, was the one corresponding to the species less the Cl3 atom (Fig. 3), hereafter **1'**–**3'**. Further, for each of **1'**–**3'**, the shortest SG–Te distances were formed for the ligand with the open conformation. The major structural consequence of **1'**–**3'**, with the loss of the Cl3 atom, is the almost orthogonal disposition of the remaining chloride atoms.

Table 4

Docking results for complexes formed between cathepsin S and each of **1**–**3** and the mono-anions derived from these in open and closed conformations. The selection of the best complex, namely **1'**–**3'**, for each series was made based on the shortest SG–Te distance.

Comp'd	Ligand with closed conformation		Ligand with open conformation		Ligand	Second order inactivation rate constant k $(mM)^{-1}$ s^{-1} [21]
	SG–Te (Å)	Energy (kcal/mol)	Energy (kcal/mol)	SG–Te (Å)		
1	3.99	−51.3	−52.0	3.39	**1**	24.5 ± 4.3
	3.86	−52.1	**−54.1**	**3.15**	**1': 1 less Cl3**	
	3.98	−51.2	−55.4	3.66	**1** less Cl2	
	3.94	−49.0	−53.7	3.21	**1** less Cl1	
2	4.22	−53.2	−52.0	3.04	**2**	1000 ± 125
	3.39	−48.2	**−52.7**	**2.99**	**2': 2** less Cl3	
	4.07	−49.5	−43.4	3.11	**2** less Cl2	
	4.19	−49.4	−45.7	3.09	**2** less Cl1	
3	3.80	−44.1	−45.6	3.54	**3**	8.7 ± 0.7
	3.62	−43.9	**−45.1**	**2.92**	**3': 3** less Cl3	
	3.90	−49.6	−45.1	3.47	**3** less Cl2	
	3.73	−45.5	−44.3	3.74	**3** less Cl1	

The analysis of the poses obtained from the docking calculations for compounds **1'**–**3'** are shown in Table 5. In Fig. 8a and 8b are shown the C–H···π interactions of formed by ligand **2'** with Phe70 and His164 of subsites S3 and S1', respectively, being representative of the analogous interactions with **1'**, and in Fig. 8c, the C=O···π interaction of **2'** with Asn163 of the S2 subsite, being representative of analogous interactions formed by **1'** and **3'**.

Table 5 Amino acids in subsites of cathepsin S that interact with ligands **1'**–**3'**. The blocks highlighted in yellow indicates a π-interaction

Subsite / Ligand	S1							S2			S3			S1′
	Asn19	Gly23	Cys25	Trp26	Asn67	Gly68	Gly69	Met71	Val162	Asn163	Gly62	Lys64	Phe70	His164
1'		X	X			X		X		X	X	X	X	X
2'		X	X	X	X	X	X		X	X	X	X	X	X
3'	X	X	X			X	X		X	X				

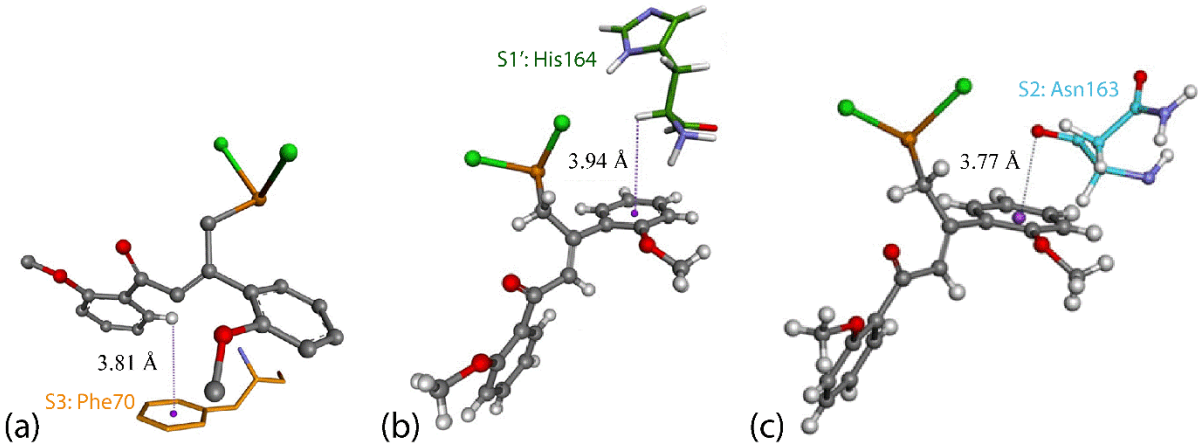

Fig. 8. C–H···π interactions of **2'** with (a) with Phe70, (b) His164 and (c) Asn163, highlighting C–H···π (a and b) and C=O···π interactions (c).

As mentioned earlier, the best inhibitors of cathepsin S should occupy subsites S2 and S3 [24]. As observed in Table 5, **3'** forms significantly less interactions in these subsites that either of **1'** and **2'**, providing a clear distinction between the ligands and the significantly reduced potency of **3'**, Table 4. As observed from Fig. 9, where the van der Waals surfaces are shown for **1'** and **2'**, ligand **2'** occupies a larger space in subsite S3 than **1'**. This and the specific interactions with crucial amino acids, as detailed below, supports the greater inhibition exhibited by **2'** over **1'**.

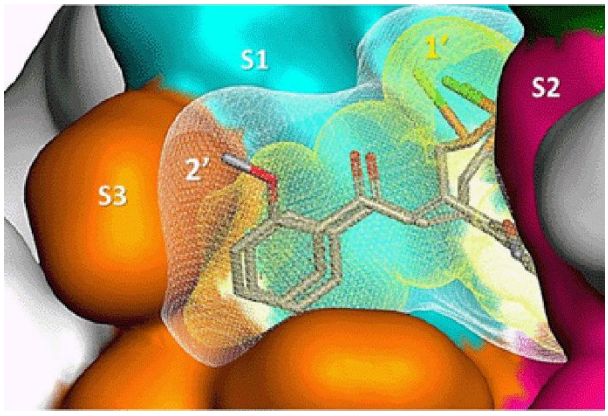

Fig. 9. Cathepsin S subsites S1 (blue), S1' (green; top right-hand corner), S2 (pink) and S3 (orange) and the van der Waals' surfaces of **1'** in yellow and **2'** in white.

The structure of cathepsin S shows that the catalytic cysteine, Cys25, is located at the end of a channel flanked by two β-strands, one of which contains the amino acid residues Val162, Asn163 and His164 and the other having Phe70 and Met71. The docking calculations show that ligands **1'** and **2'** are located between the β-strands as illustrated in Fig. 10. Fig. 10b highlights the interaction of **2'** with Val162 which has the effect of blocking the entrance of the channel giving access to the catalytic cysteine Cys25; the analogous interaction with **1'** is not apparent. This observation enables the postulate that this interaction

between **2'** and Val162 in the crucial S3 subsite is a key explanation for **2'** being more active than **1'**.

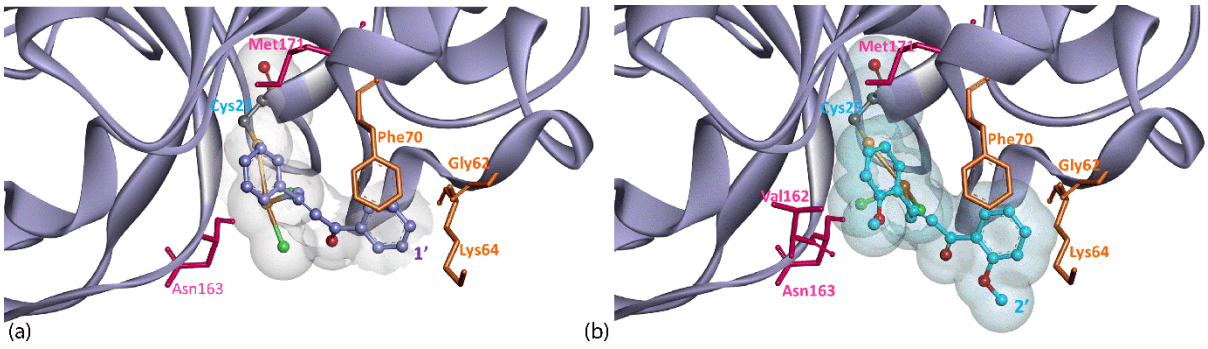

Fig. 10. Docking of (a) **1'** and (b) **2'**, shown in ball and stick form within its van der Waals' surface, in the catalytic cavity of cathepsin S.

4. Conclusions

The coordination geometry around the tellurium atom in each of **1**–**3** has been established by X-ray crystallography to be distorted ψ-pentagonal-bipyramidal with two chloride anions occupying the axial positions and with the pentagonal plane defined by the methylene-carbon and carbonyl-oxygen atoms of the chelating ligand as well and a weakly associated chloride atom derived from a neighbouring molecule; the geometry is completed by the stereochemically active lone-pair of electrons. Molecular docking studies on anions derived from **1**–**3** provides a clear explanation of the potent inhibitory behaviour of **2** with respect to the other compounds. The calculations show **2'** blocks the channel that gives access to the catalytic Cys25 site and further, **2'** occupies both the S2 and S3 subsites.

Credit author statement

Stella Hernandes Maganhi: execution of the initial docking calculations (Ph.D. student)

Ignez Caracelli: conceptualisation, execution and interpretation of the docking calculations

Julio Zukerman-Schpector: crystallography, writing, interpretation of calculations

Edward R.T. Tiekink: supramolecular calculations, writing, reviewing and editing

Rodrigo L.O.R. Cunha: synthesis and crystallisation

Mauricio Angel Veja-Teijido: earlier stages of crystal and docking studies (Ph.D. student)

Declaration of Competing Interest

The authors declare that they have no known competing financial interests or personal relationships that could have appeared to influence the work reported in this paper.

Acknowledgements

The Brazilian agencies the Coordination for the Improvement of Higher Education Personnel, CAPES, Finance Code 001 and the National Council for Scientific and Technological Development (CNPq) are acknowledged for grants (312210/2019-1, 433957/2018-2 and 406273/2015-4) to IC, (402289/2013-7 and 487012/2012-7) to RLORC for a scholarship to SHM (140925/2009-0) and a fellowship (303207/2017-5) to JZS. RLORC also acknowledge the Multi-User Central Facilities (CEM/UFABC) for the experimental support and the Sustainable Technologies Unit of UFABC (NuTS). Sunway University Sdn Bhd is thanked for financial support of this work through Grant No. GRTIN-IRG-01-2021.

[1] E.R.T. Tiekink, Therapeutic potential of selenium and tellurium compounds: Opportunities yet unrealised. Dalton Trans. 41 (2012) 6390-6395. doi: 10.1039/C2DT12225A.

[2] H.L. Seng, E.R.T. Tiekink, Anti-cancer potential of selenium- and tellurium-containing species: opportunities abound! Appl. Organometal. Chem. 26 (2012) 655-662. doi: 10.1002/aoc.2928.

[3] D. S. Persike, R. L. O. R. Cunha, L. Juliano, I.R. Silva, F. E. Rosim, T. Vignoli, F. Dona, E. A. Cavalheiro, M. J. S. Fernandes, Protective effect of the organotelluroxetane RF-07 in pilocarpine-induced status epilepticus. Neurobiol. Dis. 31(1) (2018) 120-126. doi: 10.1016/j.nbd.2008.04.001.

[4] I. A. S. Pimentel; C. S. Paladi; S. Katz; W. A. S. Judice; R. L. O. R. Cunha; C. L. Barbieri, In Vitro and In Vivo Activity of an Organic Tellurium Compound on Leishmania (Leishmania) chagasi. PLoS One 7(11) (2012) e48780. doi: 10.1371/journal.pone.0048780.

[5] P. Du, N.E.B. Saidu, J. Intemann, C. Jacob, M. Montenarh, A new tellurium-containing amphiphilic molecule induces apoptosis in HCT116 colon cancer cells. Biochem. Biophys. Acta - Gen Sub. 1840 (2014) 1808-1816. doi: 10.1016/j.bbagen.2014.02.003.

[6] R.L. Puntel, D.S. Avila, D.H. Roos, S. Pinton, Mitochondrial Effect of organoselenium and organotellurium compounds. *Curr. Org. Chem.* 20 (2016) 198-210. doi: 10.2174/1385272819666150724234948.

[7] R.H Revanna, R.K. Panchangam, U. Bhanu, S. Doddavenkatanna, Synthesis, characterization and in vitro antioxidant activity of new chiral N-boc organotellurium compounds, $(CH_3)_3OC(O)NHCH(R)C(O)NHCH_2$-$CH_2Te$-$C_6H_4$-4-

OCH_3, containing carbamate and peptide groups. J. Braz. Chem. Soc. 27 (2016) 1157-1164. doi: 10.5935/0103-5053.20160011.

[8] A. Sena-Lopes, R.N. das Neves, F.S.B. Bezerra, M.T.D. Silva, P.C. Nobre, G. Perin, D. Alves, L. Savegnago, K.R. Begnini, F.K. Seixas, T. Collares S. Borsuk, Antiparasitic activity of 1,3-dioxolanes containing tellurium in *Trichomonas vaginali*. Biomed. Pharmacother. 89 (2017) 284-287. doi: 10.1016/j.biopha.2017.01.173.

[9] R. Mello da Rosa, B.C. Piccoli, F. D'Avila da Silva, L. Dornelles, J.B.T. Rocha, M. Souza Sonego, K. Rech Begnini, T. Collares, F.K. Seixas, O.E.D. Rodrigues, Synthesis, antioxidant and antitumoral activities of 5′-arylchalcogeno-3-aminothymidine (ACAT) derivatives. Med. Chem. Commun. 8 (2017) 408-414. doi: 10.1039/C6MD00640J.

[10] T. Paschoalin, A. Martens, A. T. Omori, F. V. Pereira, L. Juliano, L. R. Travassos, G. M. Machado-Santelli, R. L. O. R. Cunha, Antitumor effect of chiral organotelluranes elicited in a murine melanoma model. Biorg. Med. Chem.27, (2019), 2537-2545.

[11] A. M. V. Nunes, F. C. P. Andrade, L. A. Filguerias, O. A. C. Maia, R. L. O. R. Cunha, S. V. A. Rodezno, A. L. M. M. Filho, F. A. A. Carvalho, D. C. Braz, A. N. Mendes, preADMET analysis and clinical aspects of dogs treated with the Organotellurium compound RF07: A possible control for canine visceral leishmaniasis? Environ. Toxicol. Pharmacol. 80 (2020) 103470. doi: 10.1016/j.etap.2020.103470.

[12] B. Sredni, Immunomodulating tellurium compounds as anti-cancer agents. Semin. Cancer Biol. 22 (2012) 60-69. doi: 10.1016/j.semcancer.2011.12.003.

[13] L. Kalich-Philosoph, H. Roness, A. Carmely, M. Fishel-Bartal, H. Ligumsky, S. Paglin, I. Wolf, H. Kanety, B. Sredni, D. Meirow, Cyclophosphamide triggers follicle

activation and “burnout”; as101 prevents follicle loss and preserves fertility. Sci. Transl. Med. 5 (2013) 185RA62. doi: 10.1126/scitranslmed.3005402.

[14] A. Silberman, Y. Kalechman, S. Hirsch, Z. Erlich, B. Sredni, A. Albeck, The anticancer activity of organotelluranes: Potential role in integrin inactivation. ChemBioChem 17 (2016) 918-927. doi: 10.1002/cbic.201500614.

[15] B. Sredni, R.R. Caspi, A. Klein, Y. Kalechman, Y. Danziger, M. Benyaakov, T. Tamari, F. Shalit, M. Albeck, A new immunomodulating compound (AS-101) with potential therapeutic application. Nature 330 (1987) 173-176. doi: 10.1038/330173a0.

[16] A. Albeck, H. Weitman, B. Sredni, M. Albeck, Tellurium compounds: Selective inhibition of cysteine proteases and model reaction with thiols. Inorg. Chem. 37 (1998) 1704-1712. doi: 10.1021/ic971456t.

[17] M. Friedman, I. Bayer, I. Letko, R. Duvdevani, O. Zavaro-Levy, B. Ron, M. Albeck, B. Sredni, Topical treatment for human papillomavirus-associated genital warts in humans with the novel tellurium immunomodulator AS101: assessment of its safety and efficacy. Br. J. Dermatol. 160 (2009) 403-408. doi: 10.1111/j.1365-2133.2008.08853.x.

[18] T. E. Yossipof, Z.R. Bazak, D. Kenigsbuch-Sredni, R.R. Caspi, Y. Kalechman, B. Sredni, tellurium compounds prevent and reverse type-1 diabetes in NOD mice by modulating α4β7 integrin activity, IL-1β, and T regulatory cells. Front. Immunol. 10 (2019) article 979. doi: 10.3389/fimmu.2019.00979.

[19] R.L.O.R. Cunha, M.E. Urano, J.R. Chagas, P.C. Almeida, C. Bincoletto, I.L.S. Tersariol, J.V. Comasseto, Tellurium-based cysteine protease inhibitors: evaluation of novel organotellurium(IV) compounds as inhibitors of human cathepsin B. Bioorg. Med. Chem. Lett. 15 (2005) 755-760. doi: 10.1016/j.bmcl.2004.11.012.

[20] R.L.O.R. Cunha, I.E. Gouvea, L. Juliano, A glimpse on biological activities of tellurium compounds. An. Acad. Bras. Cienc. 81 (2009) 393-407. doi: 10.1590/S0001-37652009000300006.

[21] R.L.O.R. Cunha, I.E. Gouvêa, G.V.P. Feitosa, M.F.M. Alves, D. Brömme, J.V. Comasseto, I.L.S. Tersariol, L. Juliano, Irreversible inhibition of human cathepsins B, L, S and K by hypervalent tellurium compounds. Biol. Chem. 390 (2009) 1205-1212. doi: 10.1515/BC.2009.125.

[22] Y.Y. Li, J. Fang, Z.G. Ao, Cathepsin B and L inhibitors: a patent review (2010-present) Expert Opin. Ther. Pat. 27 (2017) 643-656. doi: 10.1080/13543776.2017.1272572.

[23] M. Siklos, M. BenAissa, G.R.J. Thatcher, Cysteine proteases as therapeutic targets: does selectivity matter? A systematic review of calpain and cathepsin inhibitors. Acta Pharm. Sin. B 5 (2015) 506-519. doi: 10.1016/j.apsb.2015.08.001.

[24] I. Caracelli, S.H. Maganhi, J.O. Cardoso, R.L.O.R. Cunha, M.A. Veja-Teijido, J. Zukerman-Schpector, E.R.T. Tiekink, Crystallographic and docking (Cathepsins B, K, L and S) studies on bioactive halotelluroxetanes. Z. Kristallogr. 233 (2018) 113-124. doi: 10.1515/zkri-2017-2079.

[25] L. Kramer, D. Turk, B. Turk, The future of cysteine cathepsins in disease management. Trends Pharmacol Sci. 38 (2017) 873-898. doi: 10.1016/j.tips.2017.06.003.

[26] M.Z.I. Pranjol, N. Gutowski, M. Hannemann, J. Whatmore, The Potential role of the proteases cathepsin d and cathepsin L in the progression and metastasis of epithelial ovarian cancer. Biomolecules 5 (2015) 3260-3279. doi: 10.3390/biom5043260.

[27] U. Verbovsek, U.C.J.F. Van Noorden, T.T. Lah, Complexity of cancer protease biology: Cathepsin K expression and function in cancer progression. Semin. Cancer Biol. 35 (2015) 71-84. doi: 10.1016/j.semcancer.2015.08.010.

[28] O.C. Olson, J.A. Joyce, Cysteine cathepsin proteases: regulators of cancer progression and therapeutic response. Nat. Rev. Cancer 15 (2015) 712-729. doi: 10.1038/nrc4027.

[29] B. Bian, S. Mongrain, S. Cagnol, M-J. Langlois, J. Boulanger, G. Bernatchez, J.C. Carrier, F. Boudreau, N. Rivard, Cathepsin B promotes colorectal tumorigenesis, cell invasion, and metastasis. Mol. Carcinog. 55 (2016) 671-687. doi: 10.1002/mc.22312.

[30] S. H. McDowell, S. A. Gallaher, R. E. Burden, C. J. Scott, Leading the invasion: The role of Cathepsin S in the tumour microenvironment. Biochim Biophys Acta Mol Cell Res 1867 (2020) 118781. doi: 10.1016/j.bbamcr.2020.118781.

[31] D. Brömme, P. Panwar, S. Turan, Cathepsin K osteoporosis trials, pycnodysostosis and mouse deficiency models: Commonalities and differences Expert Opin. Drug Discov. 11 (2016) 457-472. doi: 10.1517/17460441.2016.1160884.

[32] V. Stoka, V. Turk, B. Turk, Lysosomal cathepsins and their regulation in aging and neurodegeneration. Ageing Res. Rev.32 (2016) 22-37. doi: 10.1016/j.arr.2016.04.010.

[33] D. Brömme, F. Lecaille, Cathepsin K inhibitors for osteoporosis and potential off-target effects. Expert Opin. Investig. Drugs. 18 (2009) 585-600. doi: 10.1517/13543780902832661.

[34] PDB: http://www.rcsb.org/pdb/home/home.do

[35] Y.D. Ward, D.S. Thomson, L.L. Frye, C.L. Cywin, T. Morwick, M.J. Emmanuel, R. Zindell, D. McNeil, Y. Bekkali, M. Girardot, M. Hrapchak, M. DeTuri, K. Crane, D. White, S. Pav, Y. Wang, M. Hao, C.A. Grygon, M.E. Labadia, D.M. Freeman, W. Davidson, J.L. Hopkins, M.L. Brown, D.M. Spero. Design and synthesis of dipeptide

nitriles as reversible and potent cathepsin S inhibitors. J. Med. Chem. 45 (2002) 5471-5482. doi: 10.1021/jm020209i.

[36] T.A. Pauly, T. Sulea, M. Ammirati, J. Sivaraman, D.E. Danley, M.C. Griffor, A.V. Kamath, L-K. Wang, E.R. Laird, A.P. Seddon, R. Ménard, M. Cygler, V.L. Rath, Specificity determinants of human cathepsin S revealed by crystal structures of complexes. Biochemistry 42 (2003) 3203-3213. doi: 10.1021/bi027308i.

[37] B. Wiederanders, D. Broemme, H. Kirschke, N. Kalkkinen, A. Rinne, T. Paquette, P. Toothman, Primary structure of bovine cathepsin S Comparison to cathepsins L, H, B and papain. FEBS Lett. 286 (1991) 189-192. doi: 10.1016/0014-5793(91)80971-5.

[38] I. Schechter, A. Berger, On the active site of proteases. III. Mapping the active site of papain; specific peptide inhibitors of papain. Biochem. Biophys. Res. Commun. 32 (1968) 898-902. doi: 10.1016/0006-291X(68)90326-4.

[39] J.S. Ainscough, T. MacLeod, D. McGonagle, R. Brakefield, J.M. Baron, A. Alase, M. Wittmann, M. Stacey, Cathepsin S is the major activator of the psoriasis-associated proinflammatory cytokine IL-36γ. Proc. Natl. Acad. Sci. U S A, 114 (2017) E2748-E2757. doi: 10.1073/pnas.1620954114.

[40] P.K. Jadhav, M.A. Schiffler, K. Gavardinas, E.J. Kim, D.P. Matthews, M.A. Staszak, D.S. Coffey, B.W. Shaw, K.C. Cassidy, R.A. Brier, Y. Zhang, R.M. Christie, W.F. Matter, K. Qing, J.D. Durbin, Y. Wang, G.G. Deng, Discovery of cathepsin S inhibitor LY3000328 for the treatment of abdominal aortic aneurysm. ACS Med. Chem. Lett. 5 (2014) 1138-1142. doi: 10.1021/ml500283g.

[41] G. Dias-da-Silva, R. L. O. R. Cunha, M. D. Coutinho-Neto, Equilibrium between tri- and tetra-coordinated chalcogenuranes is critical for cysteine protease inhibition. J. Comput. Chem. 2021 (accepted).

[42] A. Silberman, M. Albeck, B. Sredni, A. Albeck, Ligand-substitution reactions of the tellurium compound AS-101 in physiological aqueous and alcoholic solutions. Inorg. Chem. 55 (2016) 10847-10850. doi: 10.1021/acs.inorgchem.6b02138.

[43] I. Caracelli, J. Zukerman-Schpector, S.H. Maganhi, H.A. Stefani, R. Guadagnin, E.R.T. Tiekink, 2-Chlorovinyl tellurium dihalides, (p-tol)Te[C(H)=C(Cl)Ph]X_2 for X = Cl, Br and I: variable coordination environments, supramolecular structures and docking studies in cathepsin B. J. Braz. Chem. Soc. 21(2010) 2155-2163. doi: 10.1590/S0103-50532010001100018.

[44] I. Caracelli, M. Veja-Teijido, J. Zukerman-Schpector, M.H.S. Cezari, J.G.S. Lopes, L. Juliano, P.S. Santos, J.V. Comasseto, R.L.O.R. Cunha, E.R.T. Tiekink, A tellurium-based cathepsin B inhibitor: Molecular structure, modelling, molecular docking and biological evaluation. J. Mol. Struct. 1013 (2012) 11-18. doi: 10.1016/j.molstruc.2012.01.008.

[45] C. H. Yokomizo, F. S. Pessoto, T. Prieto, R. L. O. Cunha, I. L. Nantes, Effects of Trichlorotelluro-dypnones on Mitochondrial Bioenergetics and Their Relationship to the Reactivity with Protein Thiols. Chem. Res. Toxicol. 28(6) (2015) 1167-1175. doi: 10.1021/tx5005166.

[46] C.K Huang, H. Marhold, D.H O'Brien, K.J. Irgolic, The reactions of tellurium tetrachloride with acetone. *Heteroatom Chem.* 5 (1994) 463-467. doi: 10.1002/hc.520050508C.

[47] CAD4 Express Software. Enraf-Nonius, Delft, The Netherlands, 1994.

[48] XCAD4 - CAD4 Data Reduction. Harms, K. and Wocadlo, S. XCAD-4. Program for Processing CAD-4 Diffractometer Data. University of Marburg, Germany, 1995.

[49] A. Altomare, G. Cascarano, C. Giacovazzo, A. Guagliardi, Completion and refinement of crystal structures with SIR92. J. Appl. Crystallogr. 26 (1993) 343-350. doi: 10.1107/S0021889892010331.

[50] G.M. Sheldrick, Crystal structure refinement with SHELXL. Acta Crystallogr. C71 (2015) 3-8. doi: 10.1107/S2053229614024218.

[51] L.J. Farrugia, WinGX and ORTEP for Windows: an update. J. Appl. Crystallogr. 45 (2012) 849-854. doi: 10.1107/S0021889812029111.

[52] A.L. Spek, CheckCIF validation ALERTS: what they mean and how to respond, Acta Crystallogr E76 (2020) 1-11. doi: 10.1107/S2056989019016244.

[53] K. Brandenburg, DIAMOND. Crystal Impact GbR, Bonn, Germany, 2006.

[54] G. Jones, P. Willett, R.C. Glen, A.R. Leach, R. Taylor, Development and validation of a genetic algorithm for flexible docking. J. Mol. Biol. 267 (1997) 727-748. doi: 10.1006/jmbi.1996.0897.

[55] G. Jones, P. Willett, R.C. Glen, Molecular recognition of receptor sites using a genetic algorithm with a description of desolvation. J. Mol. Biol. 245 (1995) 43-53.doi: 10.1016/S0022-2836(95)80037-9.

[56] Accelrys DS Visualizer v3.5 (http://accelrys.com/).

[57] A.W. Addison, T.N. Rao, J. Reedijk, J. van Rijn, G.C. Verschoor, Synthesis, structure, and spectroscopic properties of copper(II) compounds containing nitrogen–sulphur donor ligands; the crystal and molecular structure of aqua[1,7-bis(N-

methylbenzimidazol-2′-yl)-2,6-dithiaheptane]copper(II) perchlorate. J. Chem. Soc. Dalton Trans. (1984) 1349-1356. doi: 10.1039/DT9840001349.

[58] C.-K. Huang, D.H. O'Brien, K.J. Irgolic, E.A. Meyers, 4-Oxo-2-methylpent-2-en-1-yl tellurium trichloride, $C_6H_9Cl_3OTe$. Cryst. Struct. Commun. 11 (1982) 1593-1598.

[59] N.W. Alcock, Secondary bonding to nonmetallic elements. Adv. Inorg. Chem. Radiochem. 15 (1972) 1-58. doi: 10.1016/S0065-2792(08)60016-3.

[60] I. Haiduc, R.B. King, M.G. Newton, Stereochemical aspects of tellurium complexes with sulfur ligands: molecular compounds and supramolecular associations. Chem. Rev. 94 (1994) 301-326. doi: 10.1021/cr00026a002.

[61] E.R.T. Tiekink, Supramolecular assembly based on “emerging” intermolecular interactions of particular interest to coordination chemists. Coord. Chem. Rev. 345 (2017) 209-228. doi: 10.1016/j.ccr.2017.01.009.

[62] A. Bondi, van der Waals volumes and radii. J. Phys. Chem. 68 (1964) 441-451. doi: 10.1021/j100785a001.

[63] R.L.O.R. Cunha, J. Zukerman-Schpector, I. Caracelli, J.V. Comasseto, Revisiting the addition reaction of $TeCl_4$ to alkynes: The crystal structure and docking studies of 1-chloro-2-trichlorotelluro-3-phenyl-propen-2-ol. J. Organomet. Chem. 691 (2006) 4807-4815. doi: 10.1016/j.jorganchem.2006.05.055.

Highlights

- Three biologically relevant active organotellurium trichloride are studied
- The compounds differentially inhibit cathepsin S
- The molecular structures feature a common CCl_3O donor set
- Te forms a covalent bond with S of the Cys25 residue in the active site
- Molecular docking shows effective blocking of the Cys25 active site

GRAPHICAL ABSTRACT:

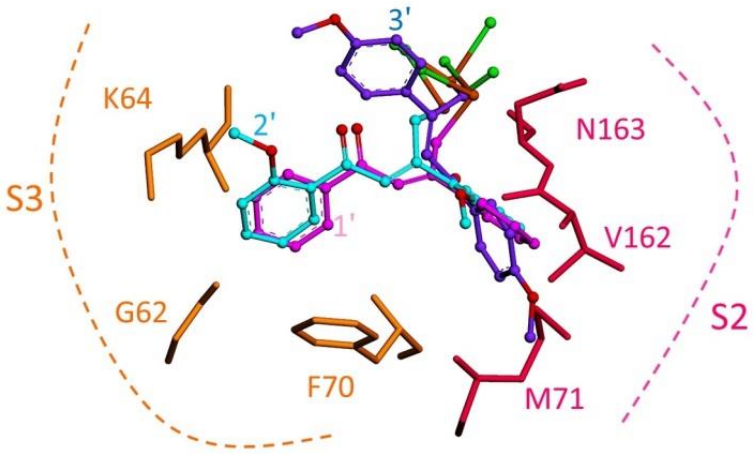

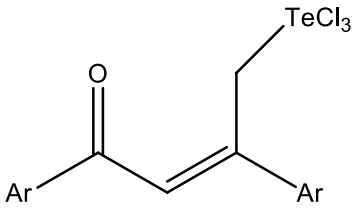

Ar = C_6H_5 (**1**), oMeO(C_6H_5) (**2**), p-MeO(C_6H_5) (**3**)
Poses of ligands after docking in CatS

Highlights

- Three biologically relevant active organotellurium trichloride are studied
- The compounds differentially inhibit cathepsin S
- The molecular structures feature a common CCl_3O donor set
- Te forms a covalent bond with S of the Cys25 residue in the active site
- Molecular docking shows effective blocking of the Cys25 active site

Scheme_1

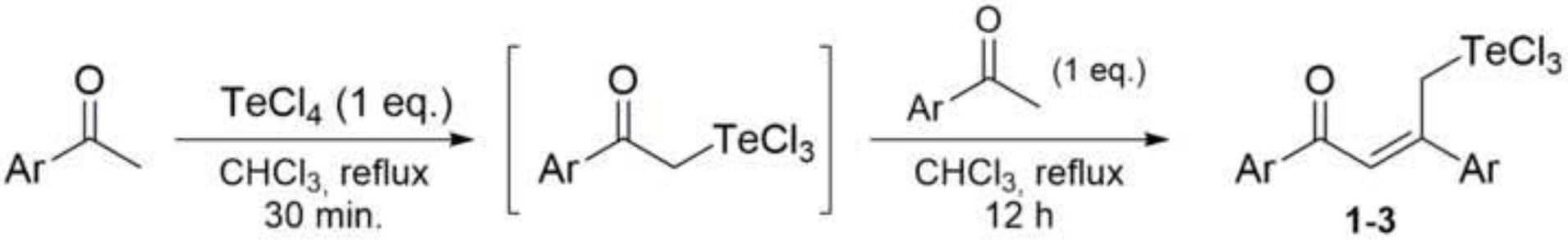

Ar = C_6H_5 (**1**, 41%), *o*-MeO(C_6H_4) (**2**, 52%), *p*-MeO(C_6H_4) (**3**, 46%)

Graphical Abstract

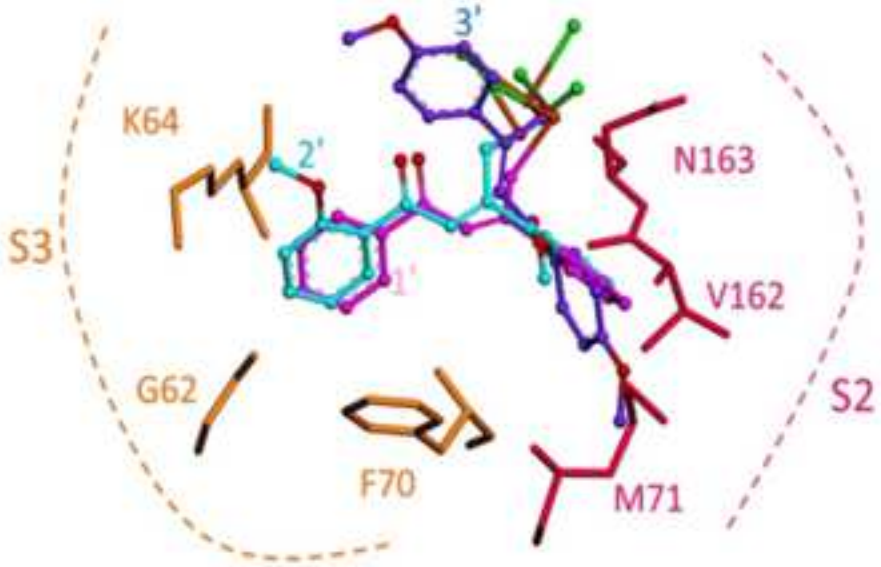

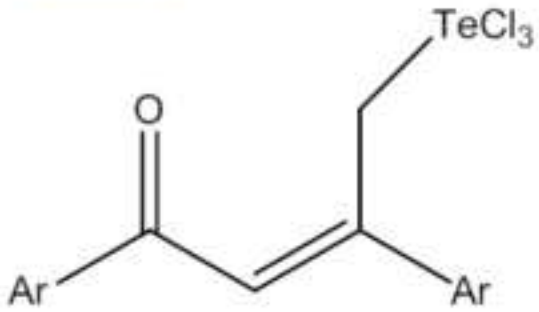

Ar = C_6H_5 (**1**), oMeO(C_6H_5) (**2**), p-MeO(C_6H_5) (**3**)

Poses of ligands after docking in CatS

Credit author statement

Stella Hernandes Maganhi: execution of the initial docking calculations (Ph.D. student)

Ignez Caracelli: conceptualisation, execution and interpretation of the docking calculations

Julio Zukerman-Schpector: crystallography, writing, interpretation of calculations

Edward R.T. Tiekink: supramolecular calculations, writing, reviewing and editing

Rodrigo L.O.R. Cunha: synthesis and crystallisation

Mauricio Angel Veja-Teijido: earlier stages of crystal and docking studies (Ph.D. student)

The authors declare that they have no competing financial interests or personal relationships that could have appeared to influence the work reported in this paper.